Organic & Biomolecular Chemistry

www.rsc.org/obc

Volume 10 | Number 48 | 28 December 2012 | Pages 9509–9752

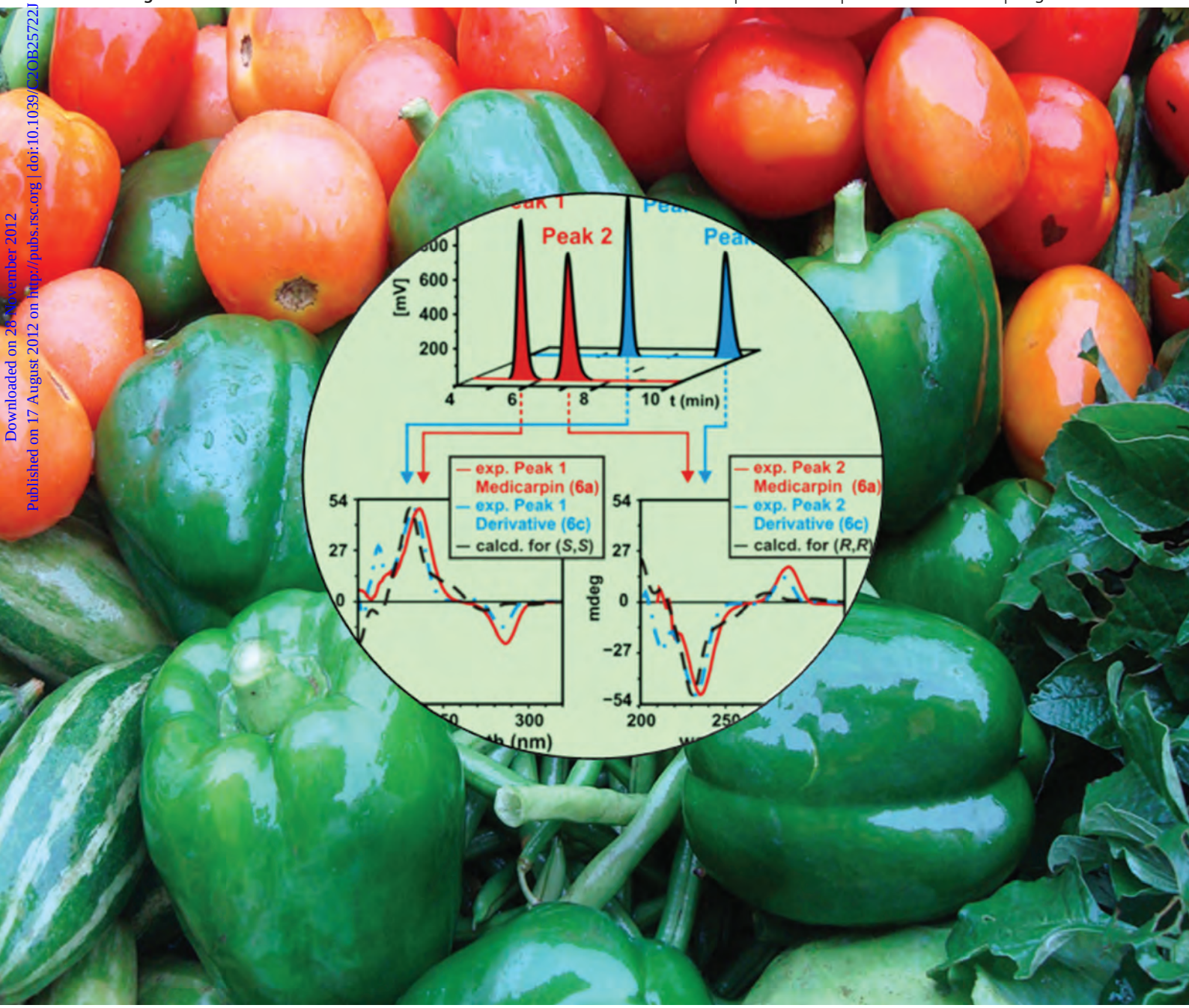

ISSN 1477-0520

RSC Publishing

PAPER

Atul Goel, Gerhard Bringmann *et al.*

Synthesis, optical resolution, absolute configuration, and osteogenic activity of *cis*-pterocarpans

Organic & Biomolecular Chemistry

Dynamic Article Links
View Article Online

Cite this: *Org. Biomol. Chem.*, 2012, **10**, 9583

www.rsc.org/obc

PAPER

Synthesis, optical resolution, absolute configuration, and osteogenic activity of *cis*-pterocarpans†

Atul Goel,*[a] Amit Kumar,[a] Yasmin Hemberger,[b] Ashutosh Raghuvanshi,[a] Ram Jeet,[a] Govind Tiwari,[a] Michael Knauer,[b] Jyoti Kureel,[c] Anuj K. Singh,[c] Abnish Gautam,[c] Ritu Trivedi,[c] Divya Singh[c] and Gerhard Bringmann*[b]

Received 4th June 2012, Accepted 16th August 2012
DOI: 10.1039/c2ob25722j

A convenient synthesis of natural and synthetic pterocarpans was achieved in three steps. Optical resolution of the respective enantiomers was accomplished by analytical and semi-preparative HPLC on a chiral stationary phase. For medicarpin and its synthetic derivative 9-demethoxymedicarpin, the absolute configuration was confirmed by a combination of experimental LC-ECD coupling and quantum-chemical ECD calculations. (−)-Medicarpin and (−)-9-demethoxymedicarpin are both 6a*R*,11a*R*-configured, and consequently the corresponding enantiomers, (+)-medicarpin and (+)-9-demethoxymedicarpin, possess the 6a*S*,11a*S*-configuration. A comparative mechanism study for osteogenic (bone forming) activity of medicarpin (racemic *versus* enantiomerically pure material) revealed that (+)-(6a*S*,11a*S*)-medicarpin (**6a**) significantly increased the bone morphogenetic protein-2 (BMP2) expression and the level of the bone-specific transcription factor Runx-2 mRNA, while the effect was opposite for the other enantiomer, (−)-(6a*R*,11a*R*)-medicarpin (**6a**), and for the racemate, (±)-medicarpin, the combined effect of both the enantiomers on transcription levels was observed.

Introduction

Pterocarpans, apart from the isoflavones, represent the second-largest group of natural isoflavonoids, with medicarpin (**6a**) and maackiain occurring almost ubiquitously.[1] They are potent phytoalexins, *i.e.*, defensive substances produced by plants in response to biotic and abiotic elicitors.[2] For example, cell suspensions of the model legume *Medicago truncatula* accumulated the isoflavonoid phytoalexin medicarpin in response to yeast elicitor or methyl jasmonate.[3,4] Depending on the producing plant, medicarpin (**6a**) was isolated either as a racemate, *e.g.*, from *Dalbergia odorifera*,[5] or in enantiomerically pure form (+)-(6a*S*,11a*S*)-medicarpin [(+)-**6a**] from *Arachis hypogea*[6] and (−)-(6a*R*,11a*R*)-medicarpin [(−)-**6a**] from *Medicago sativa*.[7]

Very few *de novo* synthetic methods to build up medicarpin have been reported in the literature. They mainly include reductive cyclisation of the corresponding isoflavone with $NaBH_4$ in THF·EtOH.[8,9] These procedures require multi-step pathways,[8] long reaction times, and often lead to poor yields.[9] Among the variety of synthetic routes to (±)-pterocarpans, the most common approaches involve the reduction and cyclisation of the corresponding 2′-hydroxyisoflavanones,[10] 1,3-Michael–Claisen annulation,[11] cycloaddition reaction of 2*H*-chromenes with 2-alkoxy-1,4-benzoquinones,[12] Heck arylation of 2*H*-chromenes with *o*-chloromercuriphenol using lithium tetrachloropalladate as a catalyst,[13] or the oxidative rearrangement of chalcones with thallium(III) nitrate.[14,15] Literature procedures for obtaining enantiomerically pure pterocarpans include resolution of racemic compounds followed by sequential functional-group modifications and/or ring transformations.[16–24] Herein we report a convenient synthesis of racemic pterocarpans, the optical resolution, and confirmation of the absolute configuration by a combination of experimental electronic circular dichroism (ECD) investigations and quantum-chemical ECD calculations, and an as yet unknown bone-forming activity of enantiomerically pure natural and synthetic pterocarpans.

Results and discussion

Our synthetic approach to the class of pterocarpan is depicted in Scheme 1. The substituted deoxybenzoins **3a–e** were synthesized

[a]*Division of Medicinal and Process Chemistry, CSIR – Central Drug Research Institute, Lucknow 226001, India. E-mail: atul_goel@cdri.res.in; Fax: +99 522 2623405*
[b]*Institute of Organic Chemistry, University of Würzburg, Am Hubland, 97074 Würzburg, Germany. E-mail: bringman@chemie.uni-wuerzburg.de; Fax: +49 931 318 4755*
[c]*Division of Endocrinology, CSIR – Central Drug Research Institute, Lucknow 226001, India*

†Electronic supplementary information (ESI) available: ^1H and ^{13}C NMR spectra of all new compounds, Cartesian coordinates of **6a** and **6c**; HPLC profile and ALP activity of **6a** and **6c**. See DOI: 10.1039/c2ob25722j

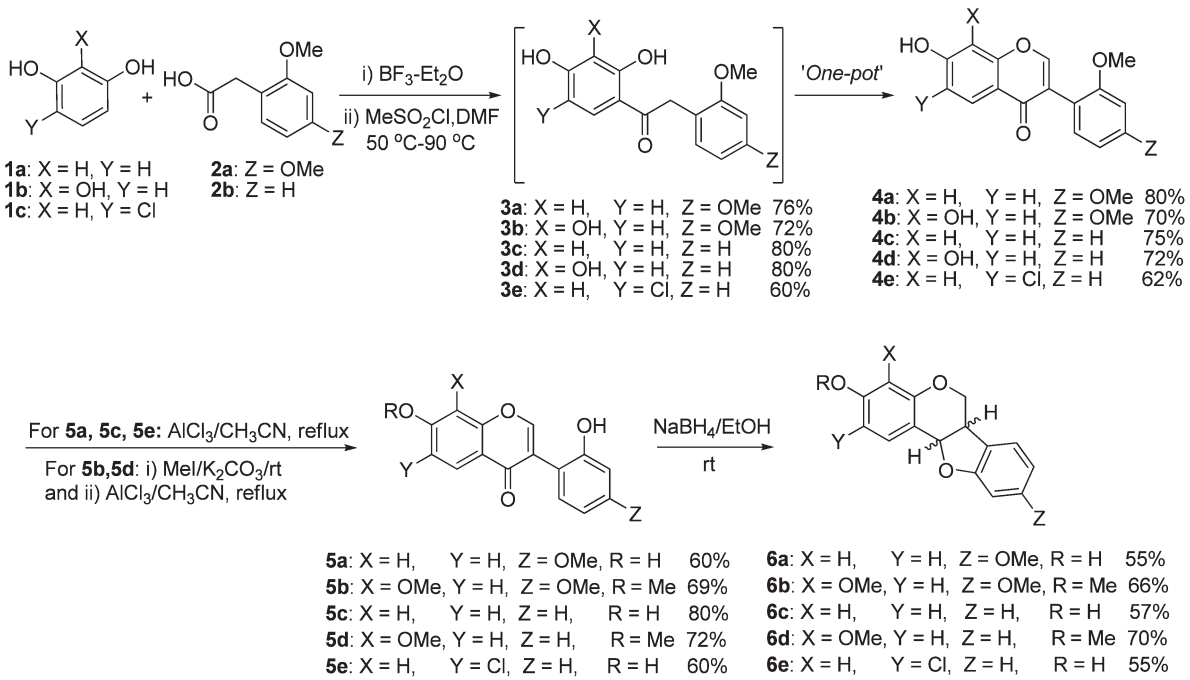

Scheme 1 Synthesis of the natural pterocarpans **6a** and **6b**, and of the synthetic analogues **6c–e**.

in situ by Friedel–Crafts acylation of the resorcinol derivatives **1a–c** and the substituted phenylacetic acids **2a** and **2b**, using $BF_3{\cdot}OEt_2$ complex solution as the reagent. The resulting reaction mixture was further treated with mesyl chloride in DMF, which led to the formation of the desired 7-hydroxy-chromen-4-one **4a–e** in good yield.[10b] Selective *O*-demethylation of **4a–e** to the 2′-hydroxyisoflavones **5a–e** was carried out successfully by $AlCl_3$ in CH_3CN.[9] Finally, pterocarpans **6a–e** were synthesized by reductive cyclisation using $NaBH_4$ in dry ethanol (see Scheme 1). The structures of the naturally occurring pterocarpans **6a** and **6b**, and of the synthetic ones **6c–e** were confirmed by spectroscopic analysis and/or by comparison with literature data.

In Nature only the *cis*-fused B/C ring system has so far been found, as present in the pterocarpans. It is energetically more favourable than the *trans*-fused ring system as demonstrated by theoretical studies.[25,26] This thermodynamical preference led to the formation of only one of the possible diastereomers of (±)-medicarpin, with its two enantiomeric forms *cis*-(6a*R*,11a*R*)- and *cis*-(6a*S*,11a*S*)-**6a**. For each of the enantiomers, two strain-free conformations of the backbone may exist; of these, the structure in which 6a-H is oriented *anti* relative to one of the hydrogen atoms at C-6 (H_{anti}, ΔE = 0.00 kcal mol^{-1}) is energetically favoured as compared to that with 6a-H *anti* to the ring oxygen (O-5) and, thus, *gauche* to both hydrogens at C-6 (O_{anti}, ΔE = 1.88 kcal mol^{-1}).[27] The calculated two main minimum conformers of the H_{anti} and of the O_{anti} backbone of *cis*-(6a*S*,11a*S*)-**6a** and *cis*-(6a*R*,11a*R*)-**6a** are shown in Fig. 1. The rapid interconversion of these two possible backbone structures at room temperature was already evidenced for related pterocarpans by Alagano and Ghio.[27]

Some of us[28,29] have developed an online HPLC-ECD method in combination with modern high-level quantum-chemical ECD calculations as a tool for the stereochemical assignment of numerous natural and synthetic chiral compounds. The first successful enantiomeric resolution of racemic pterocarpans (medicarpin and related compounds) by chiral HPLC was described by Antus *et al.*[20] and Szarvas *et al.*[18] During their experiments using methanol on Chiralpack OT(+) columns, they observed that some polymeric impurities eluted with the compounds leading to disturbances in ECD and UV measurements.[18] Therefore we developed an improved method for the resolution of the enantiomers, exemplarily elaborated for racemic medicarpin (**6a**) and for its synthetic analogue 9-demethoxymedicarpin (**6c**), to investigate the absolute configuration of synthetic and natural pterocarpans. After several attempts with different conditions on chiral stationary HPLC phases, good resolution of the enantiomers was achieved with Lux cellulose-1 (Phenomenex; 25 cm × 0.46 cm) and cellulose tris(3,5-dimethylphenylcarbamate) as the stationary phase, and a mixture of acetonitrile–water (50 : 50) as the eluent with a constant flow rate of 1 mL min^{-1} at room temperature.

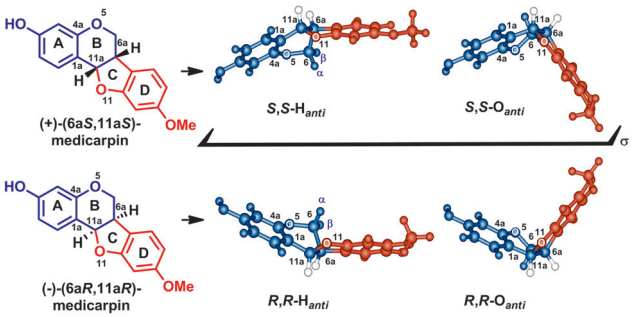

Fig. 1 Two possible configurations (left) and their two strain-free conformations of the backbone (right) of *cis*-medicarpin (**6a**).

Full LC-ECD spectra were recorded in the stopped-flow mode, leading to opposite ECD curves for the two peaks, thus confirming the assumption that these peaks indeed represented the two enantiomers of the *cis*-configured compound (**6a**). The ECD bands of the first-eluted compound showed a positive Cotton effect in the range of 210–260 nm for the ^1L_a band and a negative one in the range of 260–310 nm for the ^1L_b band, in agreement with the data reported by Szarvas *et al.*[18] Similarly, the second-eluted compound displayed exactly opposite Cotton effects as compared to the faster eluting compound. Although the relative and absolute configuration of the pterocarpans is known, based on the well established configuration of (−)-(6a*R*,11a*R*)-maackiain and the helicity rule of transition bands,[21] no direct correlation between experimental and computationally predicted CD spectra has so far been reported as a tool for the determination of the absolute configurations of natural and synthetic pterocarpans.

An attribution of the absolute configuration to the respective enantiomer of **6a** and **6c** was achieved by the combination of HPLC-ECD measurements with the quantum-chemical calculation of the ECD spectra of the respective enantiomers of **6a** and **6c**. To investigate the conformational space of (6a*R*,11a*R*)-**6a** and of (6a*R*,11a*R*)-**6c**, DFT calculations were carried out using the B3LYP[30,31] functional in combination with Pople's 6-31G* basis set.[32]

Within the energetically relevant range of 3 kcal mol^{-1} above the global minimum the conformational analysis yielded eight minimum structures for compound **6a** while for **6c** only four relevant conformers were identified, due to the missing methoxy group (see the ESI†; Table 1: Cartesian coordinates).

TDB3LYP/SV(P) calculations for these conformers, even in combination with the COSMO model[33,34] to account for solvent effects, did not permit an assignment of the absolute configuration due to an only ambiguous UV correction, which is usually an indication that the excited states are not properly calculated (not shown). Improved results were achieved using the TDB2GP-PLYP[35,36] functional with the larger Ahlrichs' TZVP[37] basis set and furthermore by a combined approach of DFT (B3LYP/SVP) and MRCI (CAS 12,12) methods.[38] It has already been proven that double-hybrid density functionals show a higher robustness and, most importantly, provide more accurate excitation energies, since excited states with charge-transfer and Rydberg-type character are described in a more balanced way as compared to the conventional density functional like B3LYP.[36] The single CD spectra calculated for the two backbone types (H_{anti} and O_{anti}) exhibited the expected difference in the CD effect, but interestingly also the orientation of the OMe function revealed a surprisingly high effect on the CD spectrum, while the arrangement of the OH group had no real impact (see the ESI; Fig. S1†). This again showed the importance of a complete analysis. All single spectra obtained were energetically weighted and summed up to give the overall UV and CD spectra. After a now unambiguous UV shift, the predicted ECD spectra were compared with the experimental ECD curves of the two resolved enantiomers.[39] Due to the strong similarity of the experimental ECD curves of the corresponding peaks of **6a** and **6c** with the calculated ones, only the calculated curves of **6a** are shown in Fig. 2, for reasons of clarity (see the ESI; Fig. S2†).

The comparison revealed good agreement between the ECD spectrum simulated for (6a*S*,11a*S*)-**6a** and the experimental one of Peak 1 (see Fig. 2b, left) and between the curve computed for (6a*R*,11a*R*)-**6a** and the online spectrum of Peak 2 (see Fig. 2b, right), thus permitting assignment of the (6a*S*,11a*S*)-configuration to the faster eluting enantiomer of **6a** and **6c** and, consequently, the (6a*R*,11a*R*)-configuration to the more slowly eluting stereoisomer of **6a** and **6c**.

Recently we have shown that isoflavonoids and pterocarpans possess osteogenic activity.[40] We found that (±)-medicarpin (**6a**) inhibits osteoclastogenesis and has non-estrogenic bone-conserving effects in ovary-ectomised mice.[41] In order to compare the osteogenic activity profile of *rac*-pterocarpan (see Table 2) with its pure enantiomers, we resolved the enantiomers of the pterocarpans **6a** and **6c** to evaluate the effect of enantiomerically pure material in two main phases of osteoblast development, *viz.* differentiation and mineralisation.

Using our chromatographic system and method (see the ESI; Fig. S3–S8†) developed for the online-ECD measurements with a semi-preparative Lux cellulose-1 column, approximately 100 mg of each, (6a*S*, 11a*S*)-**6a,c** (ee > 99.5%) and (6a*R*,11a*R*)-**6a,c** (ee > 99.5%), were obtained for evaluation of the biological activity.

Primary cultures of rat osteoblasts were used for investigating the effect of enantiomerically pure and racemic pterocarpans on osteoblast differentiation. Production of alkaline phosphatase (ALP) served as a differentiation marker of osteoblasts.[41]

An osteoblast ALP assay was used to screen the activity of enantiomerically pure and racemic pterocarpans. Briefly, calvarial osteoblasts were cultured to confluence and treated with various compounds for 48 h in the presence of ascorbate and glycerophosphate at concentrations ranging from 10^{-10} M to 10^{-6} M. At the end of the incubation period, the total ALP

Table 1 B3LYP/6-31G* relative energies of all local minima of (6a*R*,11a*R*)-medicarpin in kcal mol^{-1} depending on the backbone structure (H_{anti} or O_{anti}; φ_{ABCD}), OMe (φ_{EFGH}) and OH (φ_{IJKL}) groups arrangements

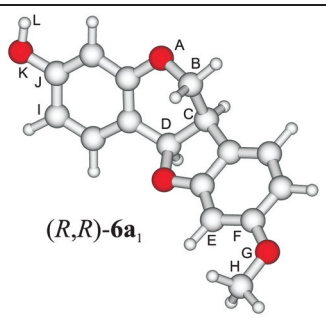

(*R*,*R*)-**6a**$_1$

Conformer	ΔE^a	φ_{ABCD} [b]	φ_{EFGH} [b]	φ_{IJKL} [b]
(*R*,*R*)-**6a**$_1$ (H_{anti})	0.00	−57	−1	−180
(*R*,*R*)-**6a**$_2$ (H_{anti})	0.16	−57	179	−180
(*R*,*R*)-**6a**$_3$ (H_{anti})	0.24	−57	−1	1
(*R*,*R*)-**6a**$_4$ (H_{anti})	0.37	−57	179	1
(*R*,*R*)-**6a**$_5$ (O_{anti})	1.88	53	0	179
(*R*,*R*)-**6a**$_6$ (O_{anti})	2.11	53	−179	179
(*R*,*R*)-**6a**$_7$ (O_{anti})	2.16	53	0	0
(*R*,*R*)-**6a**$_8$ (O_{anti})	2.30	53	−179	1

[a] Relative energies in kcal mol^{-1}. [b] Dihedral angles in degree [°].

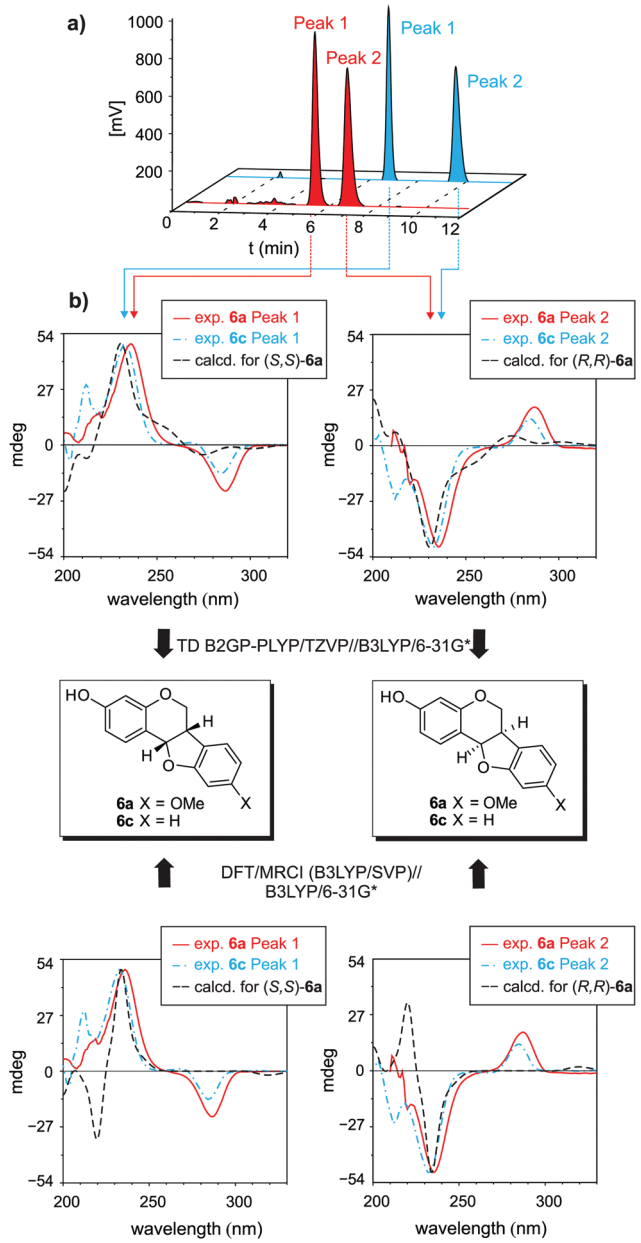

Fig. 2 Stereochemical assignment of the two enantiomers of medicarpin (**6a**) and its synthetic derivative 9-demethoxy-medicarpin (**6c**) by (a) LC-ECD coupling and quantum-chemical ECD calculations, applying (b) the TDB2GP-PLYP (above) and the combined DFT/MRCI approach (below).

activity was measured with the method using 4-nitrophenyl-phosphate (PNPP) as a substrate.[41] Treatment with the synthesised pterocarpans **6a–e**, only pterocarpans (±)-**6a,c**, (+)-**6a,c**, and (−)-**6a,c** led to increased osteoblast differentiation as assessed spectrophotometrically by osteoblast ALP production (see Table 2; see the ESI; Fig. S9–S14†).

Furthermore the effect of the respective enantiomers on the expression of osteogenic genes (Runx-2 and BMP-2) in calvarial osteoblasts by quantitative real-time PCR (qPCR) was studied. Runx-2, a bone-specific transcription factor, is a key regulator of osteoblastic differentiation.[42] Runx-2 expression is induced by

Table 2 Osteoblast differentiation and mechanism studies for osteogenic activity by pterocarpans (**6a–e**)

Compound	ALP activity[a] 10^{-10} M	10^{-8} M	10^{-6} M	BMP-2 expression[b]	Runx-2 expression[b]
(±)-**6a**	236	263	331	0.50*	0.94
(+)-**6a**	95	93	159	2.33**	2.28**
(−)-**6a**	59	73	95	1.06	2.13**
(±)-**6b**	na	na	na	—	—
(±)-**6c**	47.5	47.5	53.2	3.09**	3.50**
(+)-**6c**	58	53.2	51	1.52	10.54*
(−)-**6c**	45	51	37	1.50*	1.71**
(±)-**6d**	na	na	na	—	—
(±)-**6e**	na	na	na	—	—

[a] % increase compared with control. [b] Fold increase compared with control. 'na' means not active. *P value <0.05. **P value <0.01.

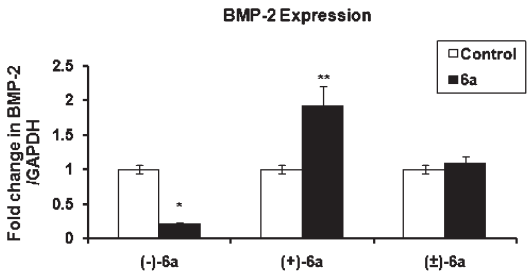

Fig. 3 mRNA levels of BMP-2 by qPCR for **6a**.

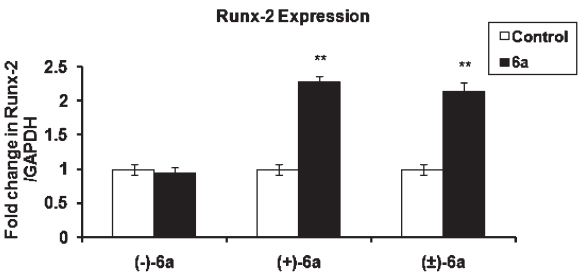

Fig. 4 mRNA levels of Runx-2 by qPCR for **6a**.

BMP-2 stimulation, suggesting that Runx-2 is a downstream transcription factor in BMP-2 signalling. Thus, mRNA levels of Runx-2 and BMP-2 were monitored by qPCR after treatment with the compounds. In the case of the medicarpins (±)-**6a**, (+)-**6a**, and (−)-**6a**, a significant increase in BMP-2 mRNA levels was found for (+)-**6a** when compared with the control (in the absence of a test substance). A decrease in the BMP-2 transcription levels was observed after treatment with (−)-**6a**, which reveals the antagonistic effect of the (6a*R*,11a*R*)-enantiomer evidencing the importance of the absolute configuration (see Fig. 3).

Runx-2 transcript levels were significantly increased by (+)-**6a** and (±)-**6a**, while for (−)-**6a** no change was observed (see Fig. 4). In the case of 9-demethoxymedicarpin [(±)-**6c**, (+)-**6c**, and (−)-**6c**)], BMP-2 and Runx-2 mRNA levels were increased for all three test substances (see Fig. 5 and 6). However, the highest increase in BMP-2 transcript level was obtained by

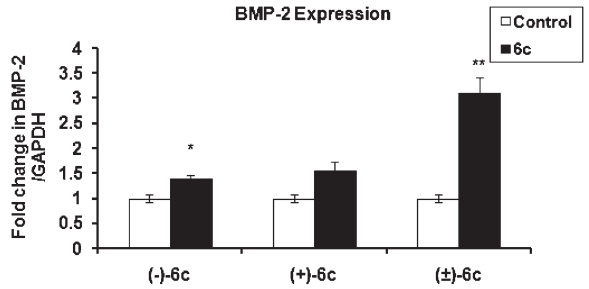

Fig. 5 mRNA levels of BMP-2 by qPCR for **6c**.

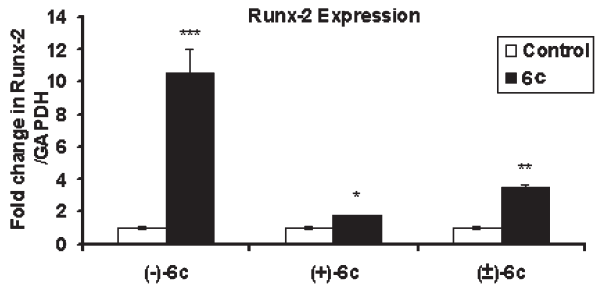

Fig. 6 mRNA levels of Runx-2 by qPCR for **6c**.

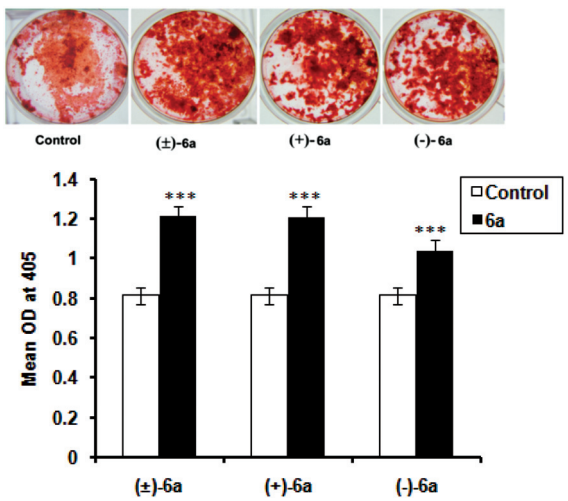

Fig. 7 Bone marrow mineralisation alizarin staining for measuring calcium nodule formation by medicarpins (±)-**6a**, (+)-**6a**, and (−)-**6a**.

treatment with (±)-**6c** possibly due to a synergistic effect of the two enantiomers. Runx-2 transcript level was maximally increased by (−)-**6c** followed by (±)-**6c**. Thus, based on ALP and qPCR, (+)-**6a** was found to be the most potent molecule among racemic and enantiomerically pure medicarpins. In addition to osteoblast differentiation, all tested compounds, (±)-**6a**, (+)-**6a**, and (−)-**6a**, promoted osteoblast mineralisation (see Fig. 7). Treatment of bone-marrow derived osteoblast cells with (±)-**6a**, (+)-**6a** or (−)-**6a** for 21 d in osteoblast differentiation media resulted in enhanced formation of mineralized nodules compared with control treated cells (see Fig. 7).

Conclusion

We have demonstrated a concise 'three-step' synthesis of the pterocarpan class of compounds. We developed an improved analytical and semi-preparative HPLC protocol for the resolution of racemates **6a** and **6c** using cellulose tris(3,5-dimethyl-phenylcarbamate) as a chiral stationary phase. The exemplary optical resolution of medicarpin (**6a**) and 9-demethoxymedicarpin (**6c**) was achieved by HPLC on a chiral phase and the absolute configuration of the respective *cis*-enantiomers was determined by LC-ECD coupling in combination with quantum-chemical ECD calculations. The comparison revealed quite good agreement between the simulated ECD spectra (calculated with TDB2GP-PLYP and MRCI) and the experimental ones, thus permitting assignment of the (6a*S*,11a*S*)-configuration to the faster eluting enantiomers of **6a** and **6c**, and consequently the (6a*R*,11a*R*)-configuration to the slower ones of **6a** and **6c**. An osteogenic study comparing racemic pterocarpans with enantiomerically pure ones showed that (6a*S*,11a*S*)-medicarpin [(+)-**6a**] significantly increased both BMP-2 and Runx-2 mRNA levels.

In short, the work described in this paper thus provides a short and efficient synthesis of racemic *cis*-pterocarpans and a new protocol for the resolution of their enantiomers on a chiral phase through analytical and preparative HPLC, and demonstrates direct correlation between experimental and computationally predicted ECD spectra as a powerful tool for the comprehensive stereochemical characterization of these bioactive substances in general.

Experimental section

Commercial reagents were used without purification. ^{1}H and ^{13}C NMR spectra were recorded at 300 MHz, with $CDCl_3$ and DMSO-d_6 as the solvents. Chemical displacements are reported in parts per million shifts (δ values) from Me_4Si (0.00 ppm for ^{1}H) or based on the central peak of the solvent $CDCl_3$ (77.00 ppm for ^{13}C NMR) as the internal standard. Signal patterns are indicated as s, singlet; d, doublet; t, triplet; m, multiplet. Coupling constants (J values) are given in Hertz (Hz). Infrared (IR) spectra were recorded on a Perkin-Elmer AX-1 spectrophotometer in a KBr disc and are reported in wave number (cm^{-1}). For mass spectra analysis, an ESI-MS spectrometer was used. Optical rotations were measured on a Rudolf Autopol III.

Experimental procedures and characterization data

1-(2,4-Dihydroxyphenyl)-2-(2,4-dimethoxyphenyl)ethanone (3a). A mixture of resorcinol (**1a**) (4.95 g, 45.0 mmol), 2-(2,4-dimethoxyphenyl)acetic acid (**2a**) (7.25 g, 37.0 mmol), and $BF_3{\cdot}OEt_2$ complex solution (12 mL) was heated at 90–100 °C for 2 h and quenched with 500 mL of water. The resulting mixture was extracted with $CHCl_3$ (3 × 75 mL) and the combined organic extracts were washed with brine, dried over anhydrous Na_2SO_4, and concentrated *in vacuo*. The crude residue was purified by silica gel column chromatography ($CHCl_3$–*n*-hexane, 4 : 1) giving **3a** (8.09 g, 76%) as a white solid, mp 150–152 °C (from $CHCl_3$–*n*-hexane) (lit.,[8] mp 154 °C); IR (KBr): ν_{max}/cm^{-1} 3261br (OH), 1635s (CO); ^{1}H NMR δ_H

(300 MHz; $CDCl_3$ + DMSO-d_6; Me_4Si) 3.61 (3 H, s), 3.62 (3 H, s), 3.98 (2 H, s), 6.11 (1 H, s), 6.23 (1 H, d, *J* 10.5), 6.28–6.38 (2 H, m), 6.90 (1 H, d, *J* 9.5), 7.69 (1 H, d, *J* 8.6), 10.39 (1 H, s, OH, D_2O exchange); ^{13}C NMR δ_C (75 MHz; $CDCl_3$ + DMSO-d_6) 200.6, 163.2, 163.1, 158.2, 156.2, 131.0, 129.5, 113.9, 110.6, 106.5, 102.9, 101.0, 96.6, 53.7, 53.4, 36.5; MS (ESI) *m*/*z* 289 ($[M + H]^+$).

1-(2,3,4-Trihydroxyphenyl)-2-(2,4-dimethoxyphenyl)ethanone (3b). The compound was prepared from benzene-1,2,3-triol (**1b**) (5.67 g, 45.0 mmol) and 2-(2,4-dimethoxyphenyl)acetic acid (**2a**) (7.25 g, 37.0 mmol) as described for **3a**, and purified by silica gel column chromatography ($CHCl_3$–*n*-hexane, 9 : 1) furnishing **3b** (8.10 g, 72%) as a white solid, mp 130–132 °C (from EtOH) (lit.,[43] mp 134–135 °C); IR (KBr): ν_{max}/cm^{-1} 3459br (OH), 1613s (CO); ^1H NMR δ_H (300 MHz; DMSO-d_6; Me_4Si) 3.63 (3 H, s), 3.67 (3 H, s), 4.08 (2 H, s), 6.35 (1 H, d, *J* 8.7), 6.40 (1 H, d, *J* 8.3), 6.47 (1 H, d, *J* 9.0), 6.98 (1 H, d, *J* 9.0), 7.38 (1 H, d, *J* 9.0), 8.58 (1 H, s, OH, D_2O exchange), 10.03 (1 H, s, OH, D_2O exchange), 12.45 (1 H, s, OH, D_2O exchange); ^{13}C NMR δ_C (75 MHz; DMSO-d_6) 203.2, 159.8, 158.0, 152.4, 152.4, 132.4, 131.5, 122.5, 115.7, 112.7, 107.8, 104.7, 98.4, 55.5, 55.2, 38.3; HRMS (ESI) exact mass calcd for $C_{16}H_{16}O_6$: 305.1025 ($[M + H]^+$). Found: 305.1000 ($[M + H]^+$).

1-(2,4-Dihydroxyphenyl)-2-(2-methoxyphenyl)ethanone (3c). The compound was prepared as described for **3a** starting from resorcinol (**1a**) (4.95 g, 45.0 mmol) and 2-(2-methoxyphenyl) acetic acid (**2b**) (6.15 g, 37.0 mmol), and purified by silica gel column chromatography ($CHCl_3$–*n*-hexane, 9 : 1) furnishing **3c** (7.66 g, 80%) as a white solid, mp 158–160 °C (from $CHCl_3$–*n*-hexane) (lit.,[44] mp 193 °C); IR (KBr): ν_{max}/cm^{-1} 3284br (OH), 1631s (CO); ^1H NMR δ_H (300 MHz; $CDCl_3$; Me_4Si) 3.80 (3 H, s), 4.23 (2 H, s), 6.33–6.42 (2 H, m), 6.86–6.98 (2 H, m), 7.19 (1 H, d, *J* 5.9), 7.24–7.32 (1 H, m), 7.83 (1 H, d, *J* 7.9), 12.68 (1 H, s, OH, D_2O exchange); ^{13}C NMR δ_C (75 MHz; $CDCl_3$) 202.6, 165.3, 162.5, 132.8, 131.0, 128.6, 123.1, 120.7, 118.9, 118.4, 110.5, 107.7, 103.5, 55.4, 39.1; MS (ESI): *m*/*z* 259 ($[M + 1]^+$).

2-(2-Methoxyphenyl)-1-(2,3,4-trihydroxyphenyl)ethanone (3d). The compound was prepared as described for **3a** using benzene-1,2,3-triol (**1b**) (5.67 g, 45.0 mmol) and 2-(2-methoxyphenyl) acetic acid (**2b**) (6.15 g, 37.0 mmol) as the starting materials, and purified by silica gel column chromatography ($CHCl_3$–*n*-hexane, 4 : 1) giving **3d** (8.11 g, 80%) as a white solid, mp 132–134 °C (from $CHCl_3$–*n*-hexane); IR (KBr): ν_{max}/cm^{-1} 3402br (OH), 1629s (CO); ^1H NMR δ_H (300 MHz; DMSO-d_6; Me_4Si) 3.76 (3 H, s), 4.20 (2 H, s), 6.41 (1 H, d, *J* 9.0), 6.85–6.90 (2 H, m), 7.12 (1 H, d, *J* 7.3), 7.19–7.25 (1 H, m), 7.38 (1 H, d, *J* 9.0), 9.83 (1 H, s, OH, D_2O exchange); ^{13}C NMR δ_C (75 MHz; DMSO-d_6) 202.5, 156.9, 152.2, 152.1, 132.2, 130.7, 128.1, 123.3, 122.1, 120.1, 112.6, 110.4, 107.6, 55.1, 38.6; HRMS (ESI) exact mass calcd for $C_{15}H_{15}O_5$: 275.0919 ($[M + H]^+$). Found: 275.0761 ($[M + H]^+$).

1-(5-Chloro-2,4-dihydroxyphenyl)-2-(2-methoxyphenyl)ethanone (3e). The compound was prepared as described for **3a** using 4-chlorobenzene-1,3-diol (**1c**) (6.50 g, 45.0 mmol) and 2-(2-methoxyphenyl)acetic acid (**2b**) (6.15 g, 37.0 mmol) as the reactants, and purified by silica gel column chromatography ($CHCl_3$–*n*-hexane 7 : 3) giving **3e** (6.46 g, 60%) as a white solid, mp 148–150 °C (from *n*-hexane–$CHCl_3$); IR (KBr): ν_{max}/cm^{-1} 1702s (CO); ^1H NMR δ_H (300 MHz; $CDCl_3$; Me_4Si) 3.83 (3 H, s), 4.19 (2 H, s), 6.24 (1 H, s), 6.49 (1 H, s), 6.81–6.98 (2 H, m), 7.16–7.31 (2 H, m), 7.98 (1 H, s, OH, D_2O exchange), 12.45 (1 H, s, OH, D_2O exchange); ^{13}C NMR δ_C (75 MHz; $CDCl_3$) 202.0, 163.9, 157.6, 156.8, 131.1, 130.9, 128.8, 122.5, 120.8, 114.2, 111.0, 110.7, 104.5, 55.4, 39.2; HRMS (ESI) exact mass calcd for $C_{15}H_{14}ClO_4$: 293.0581 ($[M + H]^+$). Found: 293.0473 ($[M + H]^+$).

General procedure for the synthesis of compounds (4a–e)

Method A. A mixture of resorcinol (**1a–c**, 45.0 mmol), 2-(2,4-dimethoxyphenyl)acetic acid (**2a**, 37.0 mmol) or 2-(2-methoxyphenyl)acetic acid (**2b**, 37.0 mmol), and $BF_3{\cdot}OEt_2$ complex solution (27 mL, 225.0 mmol) was heated at 90–100 °C for 2 h and mesyl chloride (20.7 mmol) was gradually added to it at 50 °C. The solution was then heated up to 80–90 °C for 3–4 h. After concentration of the mixture *in vacuo* the residue was treated with ice and the solid obtained was purified by silica gel column chromatography ($CHCl_3$–MeOH, 99 : 1) affording **4a–e**.

Method B. $BF_3{\cdot}OEt_2$ complex (3.5 mL, 27.6 mmol) was gradually added to a solution of deoxybenzoins (**3a–e**, 6.9 mmol) in DMF at 0 °C. The resulting solution was stirred for 30 min. After addition of mesyl chloride (1.6 mL, 20.7 mmol) at 50 °C, the solution was heated up to 80–90 °C for 5 h. The mixture was then concentrated, the residue treated with ice, and the solid obtained was purified by silica gel column chromatography ($CHCl_3$–MeOH, 99 : 1) giving **4a–e**.

*3-(2,4-Dimethoxyphenyl)-7-hydroxy-4*H*-chromen-4-one (4a).* Following the procedure described in Method A, compound **4a** (1.65 g, 80%) was isolated as a white solid, mp 238–240 °C (from $CHCl_3$–MeOH) (lit.,[8] mp 265–267 °C); IR (KBr): ν_{max}/cm^{-1} 1621s (conj. CO); ^1H NMR δ_H (300 MHz; $CDCl_3$ + DMSO-d_6; Me_4Si) 3.58 (3 H, s), 3.65 (3 H, s), 6.66 (1 H, d, *J* 2.7), 6.73 (1 H, d, *J* 2.7, 8.4), 7.00 (1 H, d, *J* 10.3), 7.71 (1 H, s), 7.81 (1 H, d, *J* 10.3); ^{13}C NMR δ_C (75 MHz; $CDCl_3$ + DMSO-d_6) 174.5, 161.6, 159.9, 157.9, 157.5, 152.7, 131.1, 126.3, 120.6, 116.1, 114.1, 112.6, 103.5, 101.4, 97.7, 54.6, 54.3; HRMS (ESI) exact mass calcd for $C_{17}H_{15}O_5$: 299.09195 ($[M + H]^+$). Found: 299.09241 ($[M + H]^+$).

*3-(2,4-Dimethoxyphenyl)-7,8-dihydroxy-4*H*-chromen-4-one (4b).* Following the procedure described in Method B, compound **4b** (1.52 g, 70%) was obtained as a white solid, mp 212–218 °C (from $CHCl_3$–MeOH) (lit.,[8] mp 238–239 °C); IR (KBr): ν_{max}/cm^{-1} 3496br (OH), 1652s (conj. CO); ^1H NMR δ_H (300 MHz; DMSO-d_6; Me_4Si) 3.64 (3 H, s), 3.73 (3 H, s), 6.50 (2 H, dd, *J* 8.4, 2.3), 6.56 (1 H, d, *J* 2.2), 6.88 (1 H, d, *J* 8.7), 7.34 (1 H, d, *J* 8.7), 8.10 (1 H, s); ^{13}C NMR δ_C (75 MHz; $CDCl_3$ + DMSO-d_6) 175.4, 161.1, 159.0, 154.2, 150.4, 147.3, 133.4, 132.6, 121.4, 117.9, 116.0, 114.5, 114.1, 105.1, 99.1, 56.0, 55.7; HRMS (ESI) exact mass calcd for $C_{17}H_{14}O_6$: 315.08686 ($[M + H]^+$). Found: 315.0871 ($[M + H]^+$).

*7-Hydroxy-3-(2-methoxyphenyl)-4*H*-chromen-4-one (4c).* Following the procedure described in Method A, compound **4c** (1.39 g, 75%) was delivered as a white solid, mp 222–224 °C

(from $CHCl_3$–MeOH); IR (KBr): ν_{max}/cm^{-1} 1628s (conj. CO); ^1H NMR δ_H (300 MHz; DMSO-d_6; Me_4Si) 3.60 (3 H, s), 7.83 (1 H, d, *J* 8.9), 7.76 (1 H, s), 7.06–7.22 (2 H, m), 6.65–6.85 (4 H, m); ^{13}C NMR δ_C (75 MHz; DMSO-d_6) 173.7, 161.4, 156.6, 156.2, 152.5, 130.4, 128.2, 126.0, 120.6, 119.9, 118.9, 115.7, 113.8, 109.8, 101.1, 54.3; HRMS (ESI) exact mass calcd for $C_{16}H_{13}O_4$: 269.08138 ($[M + H]^+$). Found: 269.07974 ($[M + H]^+$).

*7,8-Dihydroxy-3-(2-methoxyphenyl)-4*H*-chromen-4-one* ***(4d)***. Following the procedure described in Method B, compound **4d** (1.56 g, 72%) was produced as a white solid, mp 192–194 °C (from $CHCl_3$–MeOH); IR (KBr): ν_{max}/cm^{-1} 1595s (conj. CO); ^1H NMR δ_H (300 MHz; $CDCl_3$ + DMSO-d_6; Me_4Si) 3.59 (3 H, s), 6.83–6.90 (2 H, m), 6.96 (1 H, d, *J* 9), 7.10–7.13 (1 H, m), 7.23–7.32 (2 H, m), 8.10 (1 H, s), 9.38 (1 H, s, OH), 10.25 (1 H, s, OH); ^{13}C NMR δ_C (75 MHz; $CDCl_3$ + DMSO-d_6) 172.8, 156.6, 152.7, 148.9, 146.1, 132.0, 130.9, 128.7, 120.6, 120.3, 119.4, 117.1, 115.4, 113.4, 110.3, 54.7; HRMS (ESI) exact mass calcd for $C_{17}H_{14}O_6$: 315.08686 ($[M + H]^+$). Found: 315.0871 ($[M + H]^+$).

*6-Chloro-7-hydroxy-3-(2-methoxyphenyl)-4*H*-chromen-4-one* ***(4e)***. Following the procedure described in Method B, compound **4e** (1.29 g, 62%) was obtained as a white solid, mp 228–230 °C (from $CHCl_3$–MeOH); IR (KBr): ν_{max}/cm^{-1} 1625s (conj. CO); ^1H NMR δ_H (300 MHz; $CDCl_3$ + DMSO-d_6; Me_4Si) 3.68 (3H, s), 6.93–6.95 (1 H, m), 6.98 (2 H, s), 7.18–7.20 (1 H, m), 7.32–7.38 (1 H, m), 7.93 (1 H, s), 8.19 (1 H, s), 11.65 (1 H, s, OH, D_2O exchange); ^{13}C NMR δ_C (75 MHz; DMSO-d_6) 158.3, 157.9, 156.1, 154.8, 132.0, 130.2, 126.5, 122.3, 121.3, 120.5, 120.0, 117.4, 111.7, 101.1, 56.0; HRMS (ESI) exact mass calcd for $C_{16}H_{13}{}^{35}ClO_4$: 303.0424 ($[M + H]^+$). Found: 303.0421 ($[M + H]^+$).

*7-Hydroxy-3-(2-hydroxy-4-methoxyphenyl)-4*H*-chromen-4-one* ***(5a)***. To a solution of compound **4a** (2.00 g, 6.7 mmol) in CH_3CN (25 mL), $AlCl_3$ (2.66 g, 20.0 mmol) was added at 0 °C. After refluxing for 10–15 h the mixture was cooled and poured into ice-cooled water. The precipitated solid was filtered, washed with water and purified by silica gel column chromatography ($CHCl_3$–MeOH, 98 : 2) furnishing **5a** (1.14 g, 60%) as a white solid, mp 210–212 °C (from $CHCl_3$–MeOH) (lit.,[8] mp 212–215 °C); IR (KBr): ν_{max}/cm^{-1} 1619s (conj. CO); ^1H NMR δ_H (300 MHz; $CDCl_3$ + DMSO-d_6; Me_4Si) 3.61 (3 H, s), 6.25–6.39 (2 H, m), 6.68–6.80 (2 H, m), 6.98 (1 H, d, *J* 9.6), 7.85 (1 H, d, *J* 8.7), 7.92 (1 H, s), 10.33 (1 H, s, OH, D_2O exchange); ^{13}C NMR δ_C (75 MHz; DMSO-d_6) 175.2, 161.6, 159.4, 156.4, 155.5, 153.1, 130.2, 125.9, 120.9, 115.0, 114.1, 110.9, 104.1, 101.3, 100.8, 53.7; HRMS (ESI) exact mass calcd for $C_{16}H_{13}O_5$: 285.07630 ($[M + H]^+$). Found: 285.07820 ($[M + H]^+$).

*3-(2-Hydroxy-4-methoxyphenyl)-7,8-dimethoxy-4*H*-chromen-4-one* ***(5b)***. To a solution of compound **4b** (2.10 g, 6.7 mmol) in DMF (10 mL), K_2CO_3 (2.78 g, 20.1 mmol) and MeI (1.1 mL, 16.8 mmol) were added and the mixture was stirred for 5–6 h and then poured into ice-cold water and the solid was filtered. After dissolving the solid in CH_3CN (25 mL), $AlCl_3$ (2.66 g, 20 mmol) was added to the solution at 0 °C. The reaction mixture was refluxed for 10–15 h and then cooled and poured into ice-cooled water. The precipitated solid was filtered, washed with water and purified by silica gel column chromatography ($CHCl_3$–MeOH 98 : 2) giving **5b** (1.17 g, 69%) as a white solid, mp 170–172 °C (from $CHCl_3$–MeOH) (lit.,[43] mp 174–175 °C); IR (KBr): ν_{max}/cm^{-1} 1617s (conj. CO); ^1H NMR δ_H (300 MHz; $CDCl_3$ + DMSO-d_6; Me_4Si) 3.82 (3 H, s), 4.02 (3 H, s), 4.03 (3 H, s), 6.55 (2 H, dd, *J* 8.3, 2.5), 6.65 (1 H, d, *J* 2.7), 7.08 (1 H, d, *J* 8.6), 7.14 (1 H, d, *J* 9.7), 8.08–8.12 (2 H, m), 9.16 (1 H, s, OH, D_2O exchange); ^{13}C NMR δ_C (75 MHz; $CDCl_3$) 179.0, 162.0, 157.9, 157.0, 154.9, 150.5, 136.4, 130.3, 124.4, 121.9, 117.9, 112.8, 111.0, 107.6, 104.4, 61.7, 56.6, 55.4; HRMS (ESI) exact mass calcd for $C_{18}H_{16}O_6$: 329.10251 ($[M + H]^+$). Found: 329.1029 ($[M + H]^+$).

*7-Hydroxy-3-(2-hydroxyphenyl)-4*H*-chromen-4-one* ***(5c)***. Following the procedure of **5a**, compound **5c** (1.22 g, 80%) was obtained as a white solid, mp 196–198 °C (from $CHCl_3$–MeOH); IR (KBr): ν_{max}/cm^{-1} 1621s (conj. CO); ^1H NMR δ_H (300 MHz; $CDCl_3$; Me_4Si) 6.74–6.90 (4 H, m), 7.05 (1 H, d, *J* 7.7), 7.08–7.18 (1 H, m), 7.92 (1 H, s), 7.99 (1 H, d, *J* 9.7); ^{13}C NMR δ_C (75 MHz; $CDCl_3$ + DMSO-d_6) 178.1, 163.4, 157.8, 156.0, 155.0, 129.9, 129.7, 127.5, 123.9, 120.4, 120.3, 118.7, 116.0, 115.9, 102.1; HRMS (ESI) exact mass calcd for $C_{15}H_{11}O_4$: 255.06573 ($[M + H]^+$). Found: 255.06487 ($[M + H]^+$).

*7,8-Dimethoxy-3-(2-methoxyphenyl)-4*H*-chromen-4-one* ***(5d)***. Following the procedure of **5b**, compound **5d** (1.29 g, 72%) gave a white solid, mp 168–170 °C (from $CHCl_3$–MeOH); IR (KBr): ν_{max}/cm^{-1} 1626s (conj. CO); ^1H NMR δ_H (300 MHz; $CDCl_3$; Me_4Si) 4.02 (3 H, s), 4.03 (3 H, s), 6.94–7.02 (1 H, m), 7.07–7.20 (3 H, m), 7.31–7.40 (1 H, m), 8.07–8.12 (1 H, d, *J* 9.1), 8.16 (1 H, s), 8.85 (1 H, s, OH, D_2O exchange); ^{13}C NMR δ_C (75 MHz; $CDCl_3$) 178.8, 157.0, 156.4, 155.6, 150.4, 136.4, 130.5, 129.7, 124.5, 121.9, 120.8, 120.5, 119.5, 117.9, 111.0, 61.7, 56.5; HRMS (ESI) exact mass calcd for $C_{17}H_{14}O_5$: 299.0919 ($[M + H]^+$). Found: 299.0921 ($[M + H]^+$).

*6-Chloro-7-hydroxy-3-(2-hydroxyphenyl)-4*H*-chromen-4-one* ***(5e)***. Following the procedure of **5a**, compound **5e** (1.16 g, 60%) was synthesized as a white solid, mp > 250 °C (from $CHCl_3$–MeOH); IR (KBr): ν_{max}/cm^{-1} 1636s (conj. CO); ^1H NMR δ_H (300 MHz; $CDCl_3$ + DMSO-d_6; Me_4Si) 7.01–7.06 (1 H, t), 7.09–7.12 (1 H, d), 7.24 (1 H, s), 7.35–7.39 (2 H, t), 8.24 (1 H, s), 8.27 (1 H, s), 11.30 (1 H, s, OH, D_2O exchange); ^{13}C –NMR δ_C (75 MHz; DMSO-d_6) 174.2, 158.3, 156.1, 155.9, 155.3, 132.1, 129.8, 126.5, 122.2, 120.0, 119.4, 119.1, 117.6, 116.2, 104.1; HRMS (ESI) exact mass calcd for $C_{15}H_{10}{}^{35}ClO_4$: 289.0268 ($[M + H]^+$). Found: 289.0101 ($[M + H]^+$).

*9-Methoxy-6a,11a-dihydro-6*H*-benzo[4,5]furo[3,2-c] chromen-3-ol [(±)-****6a****]*. $NaBH_4$ (2.4 g, 63.6 mmol) was added to a stirred solution of chromen-4-one **5a** (3.01 g, 10.6 mmol) in absolute ethanol (30 mL) at 0 °C. The mixture was then stirred for 24 h at room temperature and the reaction was stopped by addition of ice-cooled water. Neutralisation of the solution with 10% hydrochloric acid delivered a white precipitate, which was washed with water and purified by silica gel column chromatography (*n*-hexane–$CHCl_3$, 1 : 20) giving **6a** (1.57 g, 55%) as a white solid, mp 184–186 °C (from *n*-hexane–$CHCl_3$) (lit.,[8] mp 194–195 °C); IR (KBr): ν_{max}/cm^{-1} 3393br (OH), 1594s, 1451, 1381, 1348, 1285, 1155, 1027; ^1H NMR δ_H (300 MHz; $CDCl_3$; Me_4Si) 3.49–3.70 (2 H, m), 3.79 (3 H, s), 4.26 (1 H, dd, *J* 4.5, 10.5), 4.97 (1 H, s, OH, D_2O exchange), 5.52 (1 H, d, *J* 6.6), 6.41–6.51 (3 H, m), 6.58 (1 H, dd, *J* 2.5, 8.4), 7.15 (1 H, d,

J 8.8), 7.41 (1 H, d, *J* 8.4); ^{13}C NMR δ_C (75 MHz; $CDCl_3$ + CD_3OD) 160.8, 160.3, 158.2, 156.3, 131.7, 124.6, 119.1, 111.1, 109.7, 106.1, 103.1, 96.6, 78.6, 66.2, 55.2, 39.2; HRMS (ESI) exact mass calcd for $C_{16}H_{15}O_4$: 271.09703 ($[M + H]^+$). Found: 271.09729 ($[M + H]^+$). Resolution of the enantiomers of (±)-**6a**: HPLC (semi-preparative, see the ESI; Fig. S3–S5†): (6a*S*,11a*S*)-**6a**: t_R = 20.1 min; $[\alpha]_D^{25}$ +78.19 (*c* 0.1 in CH_3CN) (lit.,[45] $[\alpha]_D^{25}$ +113.9 (*c* 0.23 in $CHCl_3$)). (6a*R*,11a*R*)-**6a**: t_R = 22.1 min; $[\alpha]_D^{25}$ −79.72 (*c* 0.1 in CH_3CN) (lit.,[46a] $[\alpha]_D^{25}$ −87.9° (*c* 0.5 in CH_3OH); lit.,[46b] −188 (*c* 0.1 in $CHCl_3$)).

*3,4,9-Trimethoxy-6a,11a-dihydro-6*H*-benzo[4,5]furo[3,2-c]chromene [(±)-**6b**]*. Application of the protocol described for **6a** led to compound **6b** (2.20 g, 66%) as a white solid, mp 110–112 °C (from *n*-hexane–$CHCl_3$) (lit.,[43] mp 114–115 °C); IR (KBr): ν_{max}/cm^{-1} 2929, 1615, 1497, 1466, 1282, 1106, 1027; ^{1}H NMR δ_H (300 MHz; $CDCl_3$; Me_4Si) 3.53–3.64 (2 H, m), 3.78 (3 H, s), 3.86 (3 H, s), 3.88 (3 H, s), 4.36 (1 H, dd, *J* 4.5, *J* 10.5), 5.52 (1 H, d, *J* 6.6), 6.45–6.48 (2 H, m), 6.69 (1 H, d, *J* 8.8), 7.15 (1 H, d, *J* 8.8), 7.25 (1 H, d, *J* 9.3); ^{13}C NMR δ_C (75 MHz; $CDCl_3$) 161.2, 160.7, 153.6, 149.5, 137.5, 125.7, 124.8, 119.0, 114.2, 106.4, 106.0, 97.0, 78.6, 66.8, 61.0, 56.2, 55.5, 39.5; HRMS (ESI) exact mass calcd for $C_{18}H_{18}O_5$: 315.12325 ($[M + H]^+$). Found: 315.12290 ($[M + H]^+$).

*6a,11a-Dihydro-6*H*-benzo[4,5]furo[3,2-c]chromen-3-ol [(±)-**6c**]*. Following the procedure described for **6a**, compound **6c** (1.45 g, 57%) was produced as a white solid, mp 148–152 °C (from $CHCl_3$–MeOH) (lit.,[47] mp 147–150 °C); IR (KBr): ν_{max}/cm^{-1} 3396br (OH), 1597, 1516, 1476, 1381, 1351, 1289, 1259, 1222, 1170, 1122, 1082, 1017; ^{1}H NMR δ_H (300 MHz; $CDCl_3$; Me_4Si) 3.53–3.72 (2 H, m), 4.23–4.32 (1 H, m), 5.21 (1 H, s, OH, D_2O exchange), 5.49 (1 H, d, *J* 6.4), 6.42 (1 H, d, *J* 2.3), 6.56 (1 H, dd, *J* 2.9, 8.7), 6.82–6.95 (2 H, m), 7.14–7.28 (2 H, m), 7.41 (1 H, d, *J* 8.1); ^{13}C NMR δ_C (75 MHz; $CDCl_3$) 159.3, 157.1, 156.6, 132.3, 129.3, 127.1, 124.8, 121.0, 112.5, 110.2, 109.9, 103.7, 77.7, 66.3, 40.1; HRMS (ESI) exact mass calcd for $C_{15}H_{13}O_3$: 241.08647 ($[M + H]^+$). Found: 241.08666 ($[M + H]^+$). Resolution of the enantiomers of (±)-**6c**: HPLC (semi-preparative, see the ESI; Fig. S6–S8†): (6a*S*,11a*S*)-**6c**: t_R = 17.8 min; $[\alpha]_D^{25}$ +79.75 (*c* 0.1 in CH_3CN). (6a*R*,11a*R*)-**6c**: t_R = 20.3 min; $[\alpha]_D^{25}$ −82.06 (*c* 0.1 in CH_3CN). $[\alpha]_D^{25}$ is not reported in the literature.[20]

*3,4-Dimethoxy-6a,11a-dihydro-6*H*-benzo[4,5]furo[3,2-c]chromene [(±)-**6d**]*. According to the procedure described for **6a**, compound **6d** (2.10 g, 70%) was furnished as a white solid, mp 106–108 °C (from *n*-hexane–$CHCl_3$); IR (KBr): ν_{max}/cm^{-1} 2931, 1610, 1471, 1286, 1224, 1108; ^{1}H NMR δ_H (300 MHz; $CDCl_3$; Me_4Si) 3.62–3.73 (2 H, m), 3.86 (3 H, s), 3.89 (3 H, s), 4.37–4.41 (1 H, dd, *J* 4.05, 10.3), 5.51–5.53 (1 H, d, *J* 6.8), 6.68–6.70 (1 H, d, *J* 8.6), 6.78–6.87 (2 H, m), 7.09–7.14 (1 H, m), 7.18–7.20 (2 H, m); ^{13}C NMR δ_C (75 MHz; $CDCl_3$) 159.5, 153.9, 149.7, 137.7, 129.5, 127.3, 126.0, 125.0, 121.2, 114.3, 110.4, 106.3, 78.0, 66.8, 61.3, 56.4, 40.3; HRMS (ESI) exact mass calcd for $C_{17}H_{16}O_4$: 285.11260 ($[M + H]^+$). Found: 285.11200 ($[M + H]^+$).

*2-Chloro-6a,11a-dihydro-6*H*-benzofuro[3,2-c]chromen-3-ol [(±)-**6e**]*. Following the procedure described for **6a**, compound **6e** (1.60 g, 55%) was synthesized as a white solid, mp 138–140 °C (from *n*-hexane–$CHCl_3$); IR (KBr): ν_{max}/cm^{-1} 3394br (OH), 1623, 1589, 1490, 1438, 1385, 1316, 1214, 1154, 1076, 1019, 957, 921, 883, 836, 747; ^{1}H NMR δ_H (300 MHz; $CDCl_3$; Me_4Si) 3.55–3.72 (2 H, m), 4.29 (1 H, dd, *J* 9.3, 3.3), 5.46 (1 H, d, *J* 6.4), 5.63 (1 H, s, OH, D_2O exchange), 6.62 (1 H, s), 6.81–6.96 (2 H, m), 7.14–7.28 (2 H, m), 7.51 (1 H, s); ^{13}C NMR δ_C (75 MHz; $CDCl_3$) 159.1, 155.6, 152.4, 130.8, 129.3, 126.7, 124.7, 121.1, 113.8, 113.4, 110.2, 109.5, 104.6, 66.4, 40.0; HRMS (ESI) exact mass calcd for $C_{15}H_{11}{}^{35}ClO_3$: 275.04750 ($[M + H]^+$). Found: 275.04340 ($[M + H]^+$).

Material and methods

Biological methods: reagents and chemicals

Cell culture media and supplements were purchased from Invitrogen (Carlsbad, CA) and all fine chemicals from Sigma-Aldrich (St. Louis, MO). The BMP-2 ELISA kit was provided by R&D Systems. The ECL kit was obtained from Amersham Pharmacia, USA. All antibodies for Western blot analysis were obtained from Cell Signaling Technologies (Danvers, MA). HPLC-grade acetonitrile and isopropanol were purchased from Sisco Research Laboratories (SRL) Pvt. Limited (Mumbai, India), *n*-hexane, ammonium acetate and glacial acetic acid (analytical grade) were provided by E-Merck Limited (Mumbai, India).

Culture of calvarial osteoblasts

Rat calvarial osteoblasts were obtained following our previously published protocol of sequential digestion.[41,48] Briefly, calvaria from 1- to 2-d-old *Sprague–Dawley* rats (both sexes) were pooled. After surgical isolation from the skull and removal of sutures and adherent mesenchymal tissues, calvaria were subjected to five sequential (10–15 min) digestions at 37 °C in a solution containing 0.1% dispase and 0.1% collagenase P. Cells released from the second to fifth digestions were pooled, centrifuged, resuspended, and plated in T-25 cm^2 flasks in α-MEM containing 10% FCS and 1% penicillin–streptomycin (complete growth medium).

Osteoblast differentiation

For the measurement of alkaline phosphatase (ALP) activity,[41,48] osteoblasts at ~80% confluence were trypsinised and 2 × 10^3 cells per well were seeded in 96-well plates. Cells were treated with different concentrations of the compounds for 48 h in α-MEM supplemented with 5% charcoal treated FCS, 10 mmol β-glycerophosphate, 50 μg mL^{-1} ascorbic acid and 1% penicillin–streptomycin (osteoblast differentiation medium). At the end of the incubation period, the total ALP activity was measured using *p*-nitrophenylphosphate (PNPP) as a substrate and quantified colourimetrically at 405 nm.

Mineralisation of bone marrow derived osteoblast cells

For mineralisation studies, bone marrow cells were cultured in a medium consisting of α-MEM, supplemented with 10% fetal bovine serum, 50 μg mL^{-1} ascorbic acid, and 10 μmol β-glycerophosphate. Cells were cultured with and without compounds

for 21 d at 37 °C in a humidified atmosphere of 5% CO_2 and 95% air, and the medium was changed every 48 h. After 7 d, the attached cells were fixed in 4% formaldehyde for 20 min at room temperature and rinsed once in PBS. After fixation, the specimens were processed for staining with 40 mmol alizarin red-S, which stains areas rich in nascent calcium. BMP-2 was used as a positive control. For quantification of alizarin red-S staining, 800 μL of 10% (v/v) acetic acid was added to each well, and plates were incubated at room temperature for 30 min with shaking. The monolayer, now loosely attached to the plate, was then scraped with a cell scraper and transferred with 10% (v/v) acetic acid to a 1.5 mL tube. After vortexing for 30 s, the slurry was overlaid with 500 μL mineral oil (Sigma-Aldrich), heated to exactly 85 °C for 10 min, and transferred to ice for 5 min. The slurry was then centrifuged at 20 000*g* for 15 min and 500 μL of the supernatant was removed to a new tube. Then 200 μL of 10% (v/v) ammonium hydroxide was added to neutralize the acid. In some cases, the pH was measured at this point to ensure that it was between 4.1 and 4.5. OD (405 nm) of 150 μL aliquots of the supernatant were measured in 96-well format using opaque-walled, transparent-bottomed plates.

For measuring BMP-2 production from osteoblasts, 5×10^3 cells per well were seeded in 24-well plates. Cells were exposed to 10^{-10} M pterocarpan for 48 h with or without inhibitors in α-MEM media supplemented with 5% FCS, 10 mmol β-glycerophosphate and 50 μg mL^{-1} ascorbic acid. At the end of incubation, supernatants were collected for determination of BMP-2 by ELISA as per the manufacturer's instructions. For inhibitor studies, cells were pre-treated with inhibitors 30 min prior to compound treatment.

Methodology for Runx-2 and BMP-2 expression by using q-PCR

Total RNA was extracted from the cultured cells using TRIzol® (Invitrogen, Carlsbad, CA). cDNA was synthesized from 2 μg total RNA with the Revert Aid™ H Minus first strand cDNA synthesis kit (Fermentas, Vilnius, Lithuania). SYBR green chemistry was used for quantitative determination of the mRNAs for BMP-2 and Runx-2 and a housekeeping gene, GAPDH, following an optimized protocol. The design of sense and antisense oligonucleotide primers for BMP-2 and Runx-2 was done using the Universal ProbeLibrary (Roche Diagnostics, Indianapolis, IN). The primer pair for BMP-2 (Gene Accession Number: NM_017178.1) was 5′-CGG ACT GCG GTC TCC TAA-3′ (sense) and 5′-GGG GAA GCA GCA ACA CTA GA-3′ (antisense); for Runx-2 (Gene Accession Number: NM_053470.1) the primer pair was 5′-GCC GGG AAT GAT GAG AAC TAC T-3′ (sense) and 5′-TCC GGC CTA CAA ATC TCA GAT C-3′ and for GAPDH it was 5′-CAG CAA GGA TAC TGA GAG CAA GAG-3′ (sense) and 5′-GGA TGG AAT TGT GAG GGA GAT G-3′ (antisense). For real-time PCR, the cDNA was amplified with a Light Cycler 480 (Roche Diagnostics Pvt Ltd, Indianapolis, IN). The double-stranded DNA-specific dye SYBR Green I was incorporated into the PCR buffer provided in the Light Cycler 480 SYBR Green I Master (Roche Diagnostics Pvt Ltd, Indianapolis, IN) to allow for quantitative detection of the PCR product in a 20 μL reaction volume. The temperature profile of the reaction was 95 °C for 5 min, 40 cycles of denaturation at 94 °C for 2 min, and annealing and extension at 62 °C for 30 s, extension at 72 °C for 30 s. GAPDH was used to normalize differences in RNA isolation, RNA degradation, and the efficiencies of the reverse transcription.

Computational details

Conformational analyses for **6a** and **6c** were done using the Gaussian03 software package.[49] For the geometry optimizations the B3LYP functional was chosen together with the double-zeta 6-31G* basis set. The TDDFT excited-states calculations of **6a** and **6c** were performed using the ORCA software package.[50] For the four conformers of each compound within the energetical range of 3 kcal mol^{-1}, single UV and ECD spectra were simulated with TDB2GP-PLYP/TZVP) (n_{states} = 40) with corresponding oscillator and rotational strength values from the length formalism.[51] Furthermore the excited states (n_{states} = 20) were calculated with MRCI (CAS 12,12) and the initial orbitals in these calculations were orbitals from a DFT [B3LYP/G/SV(P)] calculation, performed also with ORCA. The UV and ECD curves of **6a** and **6c** were calculated as sums of Gauss functions, centered at the wavelength of the corresponding excitations and multiplied by the respective oscillator and rotational strength values, with an empirically chosen exponential half width of 0.1 eV. Summation of the single spectra following the Boltzmann statistics yielded the overall UV and ECD curves. Before comparison with the experimental ECD spectra, a UV correction of 42 nm for the curves generated with TDB2GP-PLYP/TZVP and 34 nm for the spectra calculated with the combined approach of DFT (B3LYP/SVP) and MRCI was accomplished.[52] For Gauss curve generation, UV shifting, comparison with experimental data, and plotting, SpecDis[53] was used.

Acknowledgements

We gratefully acknowledge financial support from the Council of Scientific and Industrial Research (CSIR), New Delhi, India and the Alexander-von-Humboldt Foundation, Bonn, Germany for research support and equipment subsidy (HPLC system). Amit Kumar and Ashutosh Raghuvanshi are thankful to CSIR, New Delhi for research fellowships. The spectroscopic data provided by SAIF, CDRI is gratefully acknowledged. The CDRI communication number is 8295.

Notes and references

1 P. M. Dewick, in *The Flavonoids Advances in Research Since 1986*, ed. J. B. Harborne, Chapman and Hall, London, 1994, pp. 117–238.
2 J. A. Bailey and J. W. Mansfield, *Phytoalexins*, Wiley, New York, 1982, pp. 81–105.
3 J. L. Ingham and J. B. Harborne, *Nature*, 1976, **260**, 241–243.
4 M. Naoumkina, M. A. Farag, L. W. Sumner, Y. Tang, C. Liu and R. A. Dixon, *Proc. Natl. Acad. Sci. U. S. A.*, 2007, **104**, 17909–17915.
5 Y. Goda, F. Kiuchi, M. Shibuya and U. Sankawa, *Chem. Pharm. Bull.*, 1992, **40**, 2452–2457.
6 R. N. Strange, J. R. Ingham, D. L. Cole, M. E. Cavill, C. Edwards, C. J. Cooksey and P. Garratt, *Z. Naturforsch., J. Biosci.*, 1985, **40**, 313–316.
7 N. L. Paiva, R. Edwards, Y. Sun, G. Hrazdina and R. A. Dixon, *Plant Mol. Biol.*, 1991, **17**, 653–667.

8 W. Cocker, T. B. H. McMurry and P. A. Staniland, *J. Chem. Soc.*, 1965, 1034–1037.
9 G. Nabaei-Bidhendi and N. R. Bannerjee, *Indian J. Chem.*, 1990, **29B**, 366–368.
10 (*a*) A. V. Krishna Prasad, R. S. Kapil and S. P. Popli, *J. Chem. Soc., Perkin Trans. 1*, 1986, 1561–1564; (*b*) K. Wähälä and T. A. Hase, *J. Chem. Soc., Perkin Trans 1*, 1991, 3005–3008.
11 Y. Ozaki, K. Mochida and S. W. Kim, *J. Chem. Soc., Perkin Trans. 1*, 1989, 1219–1224.
12 T. A. Engler, J. P. Reddy, K. D. Combrink and D. Vander Velde, *J. Org. Chem.*, 1990, **55**, 1248–1254.
13 D. D. Narkhede, P. R. Iyer and C. S. R. Iyer, *Tetrahedron*, 1990, **46**, 2031–2034.
14 L. Farkas, A. Gottsegen, M. Nogradi and S. Antus, *J. Chem. Soc., Perkin Trans. 1*, 1974, 305–312.
15 A. McKillop, *Pure Appl. Chem.*, 1972, **43**, 463–479.
16 L. Kiss, T. Kurtán, S. Antus and H. Brunner, *Arkivoc*, 2003, 69–76.
17 S. Antus, T. Kurtán, L. Juhász, L. Kiss, M. Hollósi and Z. Májer, *Chirality*, 2001, **13**, 493–506.
18 S. Z. Szarvas, G. Y. Szokan, M. Hollósi, L. Kiss and S. Antus, *Enantiomer*, 2000, **5**, 535–543.
19 L. Kiss, T. Kurtán, S. Antus and A. Benyei, *Chirality*, 2003, **15**, 558–563.
20 S. Antus, R. Bauer, A. Gottsegen and H. Wagner, *J. Chromatogr.*, 1990, **508**, 212–216.
21 S. Ito, Y. Fujise and A. Mori, *J. Chem Soc., Chem. Commun.*, 1965, 595–596.
22 K. Mori and H. Kisida, *Liebigs Ann. Chem.*, 1989, 35–39.
23 L. Jiménez-González, S. Garcia-Muñoz, M. Alvarez-Corral, M. Muñoz-Dorado and I. Rodriguez-Garcia, *Chem.–Eur. J.*, 2006, **12**, 8762–8769.
24 T. A. Engler, M. A. Letavic, R. Iyengar, K. O. LaTessa and J. P. Reddy, *J. Org. Chem.*, 1999, **64**, 2391–2405.
25 D. Slade, D. Ferreira and J. P. Marais, *Phytochemistry*, 2005, **66**, 2177–2215.
26 J. L. Ingham, in *Progress in the Chemistry of Organic Natural Products*, ed. W. Herz, H. Grisebach and G. W. Kirby, Springer, New York, 1983, vol. 43, pp. 1–266.
27 G. Alagano and C. Ghio, *J. Phys. Chem. A.*, 2006, **110**, 647–659.
28 G. Bringmann, T. A. M. Gulder, M. Reichert and T. Gulder, *Chirality*, 2008, **20**, 628–642.
29 G. Bringmann, D. Goetz and T. Bruhn, in *Comprehensive Chiroptical Spectroscopy*, ed. N. Berova, P. Polavarapu, K. Nakanishi and R. W. Woody, John Wiley & Sons/Wiley-Blackwell, New York, 2012, vol. 2, 255–386.
30 A. D. Becke, *J. Chem. Phys.*, 1993, **98**, 5648–5652.
31 A. Schäfer, C. Huber and R. Ahlrichs, *J. Chem. Phys.*, 1994, **100**, 5829–5835.
32 P. C. Hariharan and J. A. Pople, *Theor. Chim. Acta*, 1973, **28**, 213–222.
33 F. Neese and G. Olbrich, *Chem. Phys. Lett.*, 2002, **362**, 170–178.
34 S. Sinnecker, A. Rajendran, A. Klamt, M. Diedenhofen and F. Neese, *J. Phys. Chem. A*, 2006, **110**, 2235–2245.
35 A. Karton, A. Tarnopolsky, J.-F. Lamere, G. C. Schatz and J. M. L. Martin, *J. Phys. Chem. A*, 2008, **112**, 12868–12886.
36 L. Goerigk, J. Moellmann and S. Grimme, *Phys. Chem. Chem. Phys.*, 2009, **11**, 4611–4620.
37 A. Schäfer, C. Huber and R. Ahlrichs, *J. Chem. Phys.*, 1994, **100**, 5829–5835.
38 F. Neese, *J. Inorg. Biochem.*, 2006, **100**, 716–726.
39 G. Bringmann, T. Bruhn, K. Maksimenka and Y. Hemberger, *Eur. J. Org. Chem.*, 2009, 2717–2727.
40 A. Goel, A. Kumar, S. Chaurasia, D. Singh, A. K. Gautam, R. Pandey, R. Trivedi, M. M. Singh, N. Chattopadhyay, L. Manickavasagam, G. K. Jain and A. K. Dwivedi, *Patent Appl.*, WO/2010/052734 dated 14 May 2010.
41 A. M. Tyagi, A. K. Gautam, A. Kumar, B. Bhargavan, K. Srivastava, R. Trivedi, D. K. Yadav, S. Saravanan, C. Pollet, M. Brazier, R. Mentaverri, R. Maurya, N. Chattopadhyay, A. Goel and D. Singh, *Mol. Cell. Endocrinol.*, 2010, **325**, 101–109.
42 M. Stock, H. Schäfer, M. Fliegauf and F. Otto, *J. Bone Miner. Res.*, 2004, **19**, 959–972.
43 V. K. Kalra, A. S. Kukla and T. R. Seshadri, *Tetrahedron*, 1967, **23**, 3221–3225.
44 M. T. Lu, H. D. Kuo, H. H. Ko and L. Teiking, *J. Agric. Food Chem.*, 2010, **58**, 10027–10032.
45 G. Belfosky, D. Percivill, K. Lewis, P. G. Tegos and J. Ekart, *J. Nat. Prod.*, 2004, **67**, 481–484.
46 (*a*) K. Ma, T. Ishikawa, H. Seki, K. Furihata, H. Ueki, S. Narimatsu, Y. Higuchi and C. Chaichantipyuth, *Heterocycles*, 2005, **65**, 893–900; (*b*) L. C. Chang, C. Gerhäuser, L. Song, N. R. Farnsworth, J. M. Pezzuto and A. D. Kinghorn, *J. Nat. Prod.*, 1997, **60**, 869–873.
47 J. C. Breytenbach, J. J. van Zyl, P. J. van der Merwe, G. J. H. Rall and D. G. Roux, *J. Chem. Soc., Perkin Trans. 1*, 1981, 2684–2691.
48 B. Bhargavan, A. Gautam, D. Singh, A. Kumar, S. Chaurasia, A. Tyagi, D. Yadav, J. Sharan, A. Singh, S. Sanyal, A. Goel, R. Maurya and N. Chattopadhyay, *J. Cell. Biochem.*, 2009, **108**, 388–399.
49 M. J. Frisch, G. W. Trucks, H. B. Schlegel, G. E. Scuseria, M. A. Robb, J. R. Cheeseman, J. J. A. Montgomery, T. Vreven, K. N. Kudin, J. C. Burant, J. M. Millam, S. S. Iyengar, J. Tomasi, V. Barone, B. Mennucci, M. Cossi, G. Scalmani, N. Rega, G. A. Petersson, H. Nakatsuji, M. Hada, M. Ehara, K. Toyota, R. Fukuda, J. Hasegawa, M. Ishida, T. Nakajima, Y. Honda, O. Kitao, H. Nakai, M. Klene, X. Li, J. E. Knox, H. P. Hratchian, J. B. Cross, V. Bakken, C. Adamo, J. Jaramillo, R. Gomperts, R. E. Stratmann, O. Yazyev, A. J. Austin, R. Cammi, C. Pomelli, J. W. Ochterski, P. Y. Ayala, K. Morokuma, G. A. Voth, P. Salvador, J. J. Dannenberg, V. G. Zakrzewski, S. Dapprich, A. D. Daniels, M. C. Strain, O. Farkas, D. K. Malick, A. D. Rabuck, K. Raghavachari, J. B. Foresman, J. V. Ortiz, Q. Cui, A. G. Baboul, S. Clifford, J. Cioslowski, B. B. Stefanov, G. Liu, A. Liashenko, P. Piskorz, I. Komaromi, R. L. Martin, D. J. Fox, T. Keith, M. A. Al-Laham, C. Y. Peng, A. Nanayakkara, M. Challacombe, P. M. W. Gill, B. Johnson, W. Chen, M. W. Wong, C. Gonzalez and J. A. Pople, *Revision D.01 ed*, Gaussian, Inc., Wallingford CT, 2004.
50 F. Neese, *ORCA version 2.9.0* (http://www.thch.uni-bonn.de/tc/orca/), University of Bonn, Bonn, 2008.
51 W. Moffit, *J. Chem. Phys.*, 1956, **25**, 467–478.
52 G. Bringmann and S. Busemann, in *Natural Product Analysis: Chromatography, Spectroscopy, Biological Testing*, ed. P. Schreier, M. Herderich, H. U. Humpf and W. Schwab Vieweg, Wiesbaden, 1998, pp. 195–211.
53 T. Bruhn, Y. Hemberger, A. Schaumlöffel and G. Bringmann, *SpecDis version 1.52*, University of Würzburg, Würzburg, 2011.

